JPET Fast Forward. Published on February 16, 2018 as DOI: 10.1124/jpet.117.245118
This article has not been copyedited and formatted. The final version may differ from this version.

Title: Targeting KCa1.1 channels with a scorpion venom peptide for the therapy of rat models of rheumatoid arthritis

Mark R. Tanner, Michael W. Pennington, Brayden H. Chamberlain, Redwan Huq, Elizabeth J. Gehrmann, Teresina Laragione, Pércio S. Gulko, and Christine Beeton

Department of Molecular Physiology and Biophysics, Baylor College of Medicine, Houston, TX 77030, USA (M.R.T., B.H.C., R.H., E.J.G., C.B.)

Interdepartmental Graduate Program in Translational Biology and Molecular Medicine, Baylor College of Medicine, Houston, TX 77030, USA (M.R.T.)

Peptides International, Inc., Louisville, KY 40299, USA (M.W.P)

Division of Rheumatology, Department of Medicine, Icahn School of Medicine at Mount Sinai, New York, NY 10029, USA (T.L., P.S.G.)

Biology of Inflammation Center and Center for Drug Discovery, Baylor College of Medicine, Houston, TX 77030, USA (C.B.)

Running title: Targeting KCa1.1 in rat models of RA

Correspondence to:

Dr. Christine Beeton

Mailing Address: One Baylor Plaza, Houston, TX 77030

Tel: (+1) 713-798-5030, Fax: (+1) 713-798-3475

E-mail: beeton@bcm.edu

Number of text pages: 31

Number of figures: 7

Number of references: 51

Number of words in abstract: 249

Number of words in introduction: 719

Number of words in discussion: 1621

Nonstandard abbreviations:

CIA	Collagen-induced arthritis
FLS	Fibroblast-like synoviocyte
IbTX	Iberiotoxin
KCa1.1	Calcium-activated potassium channel
Pax	Paxilline
PIA	Pristane-induced arthritis
RA	Rheumatoid arthritis

Recommended section assignment: Drug Discovery and Translational Medicine

Abstract

Fibroblast-like synoviocytes (FLS) are a key cell-type involved in rheumatoid arthritis (RA) progression. We previously identified the KCa1.1 potassium channel (Maxi-K, BK, Slo 1, *KCNMA1*) as a regulator of FLS and that KCa1.1 inhibition reduces disease severity in RA animal models. However, systemic KCa1.1 block causes multiple side effects and in this study, we aimed to determine whether the KCa1.1 β1-3-specific venom peptide blocker iberiotoxin (IbTX) reduces disease severity in animal models of RA without inducing major side effects. We used immunohistochemistry to identify IbTX-sensitive KCa1.1 subunits in joints of rats with a model of RA. Patch clamp and functional assays were used to determine if IbTX can regulate FLS through targeting KCa1.1. We then tested the efficacy of IbTX in ameliorating disease in two rat models of RA. Finally, we determined if IbTX causes side-effects including incontinence or tremors in rats, compared to those treated with the small molecule KCa1.1 blocker paxilline. IbTX-sensitive subunits of KCa1.1 are expressed by FLS in joints of rats with experimental arthritis. IbTX inhibits KCa1.1 channels expressed by FLS from patients with RA and by FLS from rat models of RA and reduces FLS invasiveness. IbTX significantly reduces disease severity in two rat models of RA. Unlike paxilline, IbTX does not induce tremors or incontinence in rats. Overall, IbTX inhibits KCa1.1 channels on FLS and treats rat models of RA without inducing side effects associated with non-specific KCa1.1 blockade and could become the basis for the development of a new treatment for RA.

Introduction

Rheumatoid arthritis (RA) is a chronic, systemic autoimmune disease affecting approximately 1.3 million people in the United States. It involves inflammation of the synovial joints (Helmick et al., 2008). Fibroblast-like synoviocytes (FLS) are resident synovial joint cells that play a central role in the progression of RA. These cells develop a highly invasive phenotype and secrete proteases, growth factors, and pro-inflammatory cytokines and chemokines, leading to joint degradation (Bartok and Firestein, 2010; Bottini and Firestein, 2013). This invasive phenotype is a hallmark of FLS in RA as their level of *ex vivo* invasiveness is correlated with radiography damage in patients with RA (Tolboom et al., 2005) and with histology changes in rodents (Laragione et al., 2008). Current therapeutics for RA are focused on suppressing the immune component of RA and no current therapeutics have been designed to specifically target FLS (Kahlenberg and Fox, 2011).

FLS from patients with RA (RA-FLS) and from rats with the pristane-induced arthritis (PIA) model of RA express the KCa1.1 potassium channel (Maxi-K, BK, Slo 1, *KCNMA1*) at their plasma membrane (Beeton, 2017; Hu et al., 2012; Pethő et al., 2016; Tanner et al., 2015). Inhibiting the expression or function of this channel reduces FLS invasiveness, proliferation, and protease secretion, while modulating cellular adhesion and integrin regulation (Hu et al., 2012; Tanner et al., 2015; Tanner et al., 2017a). Furthermore, blocking KCa1.1 with the small molecule inhibitor paxilline reduces disease severity in PIA and in the collagen-induced arthritis (CIA) rat models of RA (Tanner et al., 2015).

Though paxilline was efficacious at treating disease in these rat models of RA, its development as a potential therapeutic is limited by its side effects. Pore-forming α

subunits of KCa1.1 are found in a variety of tissues including the central nervous system (CNS), smooth muscle, testis, pancreas, and kidney in addition to FLS (Poulsen et al., 2009; Uebele et al., 2000). Paxilline blocks KCa1.1 through allosteric binding to the pore-forming α subunit (Sanchez and McManus, 1996) and its systemic administration leads to KCa1.1 block throughout the body, causing detrimental side effects that preclude its use in humans (Imlach et al., 2008; Meredith et al., 2004).

Though KCa1.1 α subunits have a wide tissue distribution, many KCa1.1 channels are physically associated with regulatory β subunits that affect channel gating and activation and have restricted tissue distributions. Highly invasive, $CD44^{high}$, $cadherin\text{-}11^{high}$, and $podoplanin^{high}$ RA-FLS express KCa1.1 containing the β3 subunit (Pethő et al., 2016). In contrast, KCa1.1 α in the CNS is associated with the β4 subunit while the β1 subunit is expressed in smooth muscle cells. Because of the limited tissue distribution of KCa1.1 with the β3 subunit (Mannowetz et al., 2013; Pethő et al., 2016; Poulsen et al., 2009), it may be possible to utilize a blocker that affects KCa1.1 αβ3, but not KCa1.1 αβ4, as a step towards a novel therapy of RA that would not induce side effects in the CNS and as a proof of concept that targeting specific subunits of KCa1.1 can be used for tissue-specific pharmacology.

Iberiotoxin (IbTX), a 37 amino acid peptide from the venom of the *Buthus tamulus* scorpion (Galvez et al., 1990; Yu et al., 2016), is a selective KCa1.1 blocker that inhibits the channel when it contains the β1, 2, or 3 subunits (Li et al., 2007; Lippiat et al., 2003; Löhn et al., 2001) while having no effect on KCa1.1 containing the β4 subunit found in the CNS (Wang et al., 2014). IbTX may therefore inhibit FLS through blocking KCa1.1 αβ3, while leaving the CNS unaffected by sparing KCa1.1 αβ4. If efficacious in treating

models of RA, IbTX could serve as a scaffold for the development of KCa1.1 αβ3-specific blockers for the treatment of RA.

Here, we tested the hypothesis that IbTX can be used to block KCa1.1 expressed by FLS without inducing the side effects observed with global KCa1.1 blockade. We show that IbTX blocks KCa1.1 in RA-FLS, PIA-FLS and CIA-FLS, along with reducing their *ex vivo* invasiveness. We also show that IbTX is effective at reducing disease severity in the PIA and CIA rat models of RA and that paxilline, but not IbTX, induces tremors and incontinence in rats. Taken together, our results indicate IbTX as a tool for targeting FLS without affecting other cells expressing KCa1.1, thereby reducing side effects associated with global KCa1.1 blockade.

Materials and Methods

Animals

8-11 week old female dark agouti (DA) rats (Envigo) and Lewis rats (Charles River) were housed in autoclaved cages in an AAALAC-accredited facility and given food and water *ad libitum*. All experiments involving rats were approved by the Institutional Animal Care and Use Committee at Baylor College of Medicine.

Immunohistochemistry, histology, and X-rays

Hind paws from rats with either collagen-induced arthritis (CIA) or pristane-induced arthritis (PIA) were collected 14 or 21 days after disease onset, respectively, at which time disease has been severe for a long duration and animals have noticeable significant pathologic hallmarks of disease. X-rays were taken with an In Vivo Xtreme Imaging

System (Bruker). Paws were decalcified, embedded in paraffin, sectioned, and stained for either safranin O/fast green, hematoxylin/eosin, or by immunohistochemistry. Analysis and scoring of safranin O/fast green and hematoxylin/eosin-stained samples were completed as described (Brenner et al., 2005) by an investigator blinded to treatment groups. For immunohistochemistry, sections were deparaffinized and hydrated before antigen retrieval and blocking of non-specific protein binding sites, peroxidase, and alkaline phosphatase. Sections were incubated in primary antibodies against cadherin-11 (Invitrogen MA1-06306), podoplanin (Abcam ab10288), KCa1.1 α (NeuroMab 75-022 or EMD Millipore AB5228), and KCa1.1 β3 (Invitrogen PA5-32891). For detection, we used ImmPRESS anti-mouse and anti-rabbit IgG conjugated to alkaline phosphatase and peroxidase, respectively, followed by ImmPACT DAB and Vector Red substrates (Vector Laboratories). Images of the synovial joints were taken using an Olympus Q Color 5 camera on an Olympus BX41 microscope at 10X magnification and images of synovium were taken at 40X magnification.

Cells

FLS from patients with RA, diagnosed according to criteria set forth by the American College of Rheumatology (Aletaha et al., 2010), were isolated as described (Laragione and Gulko, 2010). Rat FLS were isolated as described (Laragione et al., 2008) from the hind paws of rats with either CIA or PIA that had signs of disease for 14 or 21 days, respectively, at which time disease has been severe for a long duration. All experiments were conducted with FLS after passage 3.

Synthesis of IbTX

IbTX was synthesized on a Prelude Peptide Synthesizer (Protein Technologies, Tucson, AZ) using an Fmoc-tBu protecting strategy will all Cys residues protected as Cys(Trt). Synthesis was initiated on Fmoc-Gln(Trt)-Wang resin (Peptides International, Louisville, KY) using diisopropyl carbodiimide (DIC) /Oxyma activation chemistry. Following synthesis of the linear sequence, the final pyroglutamic acid was coupled manually also using DIC/Oxyma. The peptide was cleaved from the resin using an acidolytic cleavage cocktail (trifluoroacetic acid [TFA]: anisole: H_2O: triisopropyl silane: thioanisole; 9: 0.2: 0.2: 0.2: 0.2 v/v) for 2 hours at room temperature. Following cleavage from the resin and deprotection of the side chain residues, the crude peptide was filtered to remove the spent resin beads and precipitated into ice cold diethyl ether and washed five times with the same solvent. The crude peptide was subsequently dissolved in 50% aqueous acetic acid and diluted into water to a concentration of 0.2 mg/ml. The pH of this solution was adjusted to 7.8 with NH_4OH and glutathione was added to facilitate disulfide formation (0.1 mM GSSG and GSH). Following 18 hour oxidation, the peptide was monitored by RP-HPLC for formation of the folded peptide which shifts to a more hydrophilic retention time. The pH of the folded peptide solution was subsequently lowered with TFA to 4.0 and pumped onto a 5 x 60 cm preparative RP-HPLC column (Phenomenex Luna C18-10 u, 100 Å pore size). The folded peptide was purified using a gradient of 5 - 35% acetonitrile versus 0.05% TFA in H_2O over 90 min. The peptide fractions with a purity greater than 95% by analytical RP-HPLC were pooled and lyophilized. The final peptide was characterized by amino acid analysis and ESI-MS and

co-eluted with a reference sample of IbTX. Each batch was tested by electrophysiology for KCa1.1 block on HEK293 cells expressing KCa1.1 α.

Patch-clamp electrophysiology

FLS were lifted with trypsin-EDTA, washed and patch-clamped using a Port-a-Patch automated system (Nanion Technologies), as described (Hu et al., 2012; Pethő et al., 2016; Tajhya et al., 2016).

Measuring FLS invasiveness

Invasiveness of FLS was determined as described (Hu et al., 2012; Laragione et al., 2008).

Induction and scoring of RA models

PIA was induced in female DA rats by a subcutaneous injection of 150 µl pristane (MP Biomedicals) at the base of the tail, as described (Beeton et al., 2006; Tarcha et al., 2012). CIA was induced in female Lewis rats (Griffiths et al., 1992) by a subcutaneous injection of 200 µl of 2 mg/ml porcine type II collagen (Chondrex) in a 1:1 emulsion with incomplete Freund's adjuvant (Difco). Seven days later, rats were given a booster injection of 100 µl of the same emulsion.

Disease onset was defined by at least one swollen or red joint. Clinical scores were determined daily for each rat as described (Tarcha et al., 2012). For each rat, 5 points were given for each red or swollen ankle or wrist and 1 point for each red or swollen toe joint, with a maximum possible score of 60 for each rat. Upon disease onset, rats were

randomly assigned to receive either vehicle, IbTX subcutaneously, or paxilline intraperitoneally every other day. Randomization of rats to treatment groups was done by assigning every-other rat that developed signs of disease on a given day to the same treatment group so that each group was composed of rats that developed signs of disease across the same timeframe and without regard to basal disease severity on the day each rat had noticeable paw inflammation. The number of rats per treatment group was determined using power analysis with a power of 0.8 and an alpha of 0.5 and based off of previous experiments testing KCa1.1 blockers in rat models of RA, as described (Tanner et al., 2015).

Tremor measurements

Lewis rats were treated with either DMSO, 20 mg/kg paxilline, or 0.5 mg/kg IbTX and placed in a suspended chamber 10 minutes, 1 hour, and 24 hours after treatment. An iPhone 6 (Apple) was attached to the bottom, outer surface of the chamber and tremors were measured through the phone's built-in accelerometer with vibration measurement and recording completed with the VibSensor app (Now Instruments and Software, Inc.) (Miyazaki et al., 2014) over the course of 10 minutes. The acceleration data were root-mean-square (RMS) transformed with smoothing across 0.1 second increments, as described (Feketa et al., 2013). To determine tremor frequency over 10 minutes, a threshold above background RMS-transformed acceleration of 0.15 m/s^2 was set and a single tremor event was counted as when the RMS-transformed acceleration passed through this threshold. To determine tremor intensity, the integral of the RMS-transformed acceleration was taken for a one minute period in which the rat was not actively moving.

Rats were monitored over the course of measurements and data were excluded when a rat was moving.

Incontinence assays

Lewis rats were given either an intraperitoneal treatment of vehicle or 20 mg/kg paxilline (Fermentek, Israel), or a subcutaneous treatment of 0.5 mg/kg IbTX and then given an oral gavage of 1 ml water. They were then placed individually in paper towel-lined cages. After one hour, the number of urine spots each rat produced was counted in the dark using a black light (Meredith et al., 2004).

Statistical analysis

All data are presented as mean ± SEM. Differences between groups were determined using the Mann-Whitney U tests or matched-pairs T tests. A p value less than 0.05 was considered statistically significant.

Results

Detection KCa1.1 β3 in CIA joints

We previously found that FLS from rats with PIA express KCa1.1 and that their invasion is modulated by channel activity and expression (Tanner et al., 2015). Though, as ion channel subunit expression can differ between species and animal model (Tanner and Beeton, 2018), we assayed the *in vivo* expression of FLS expression of KCa1.1 α and β3 within the synovial paw joints of rats with CIA, using cadherin-11 and podoplanin as markers for FLS. Cadherin-11$^+$ and podoplanin$^+$ cells express KCa1.1 α and β3 in CIA

rat synovium (Fig. 1). These data indicate that FLS express KCa1.1 with the β3 subunit *in vivo* during CIA and therefore allow for the CIA rat model to be used to assess the effect of KCa1.1 blockers at targeting FLS *in vivo*.

IbTX blocks KCa1.1 channels expressed by FLS and reduces FLS invasiveness

Since the ability of IbTX to block KCa1.1 channels depends on the regulatory β subunits expressed (Wang et al., 2014) and channel sensitivity to modulators can vary between species (Tanner and Beeton, 2018), we compared its effects on potassium channels from RA-, PIA-, and CIA-FLS. IbTX blocked the potassium channels in all 3 cell types with similar IC_{50}s in the 2-10 nM range previously described for IbTX on KCa1.1 lacking β4 subunits (Meera et al., 2000; Tauc et al., 1993): 2.2 ± 0.3 nM for RA-FLS, 2.6 ± 0.7 nM for PIA-FLS, and 3.7 ± 0.8 nM for CIA-FLS (Fig. 2A).

The small molecule KCa1.1 blocker paxilline reduces the *ex vivo* invasiveness of RA- and PIA-FLS (Hu et al., 2012; Tanner et al., 2015). Similar to paxilline, IbTX significantly reduced the number of RA-, PIA-, and CIA-FLS that invaded through Matrigel-coated Transwell inserts by approximately 50% (Fig. 2B).

IbTX reduces disease severity in two rat models of RA

Upon disease onset, rats with PIA were treated with vehicle or 0.05 mg/kg, 0.5 mg/kg, or 5 mg/kg IbTX subcutaneously every other day. These doses were chosen because venom peptides with a similar structure display efficacy in blocking their ion channel target at doses of 0.1-0.5 mg/kg in animal models of RA (Beeton et al., 2006; Tanner et al., 2017b; Tarcha et al., 2012). Rats treated with IbTX exhibited a greater than 50% reduction

in arthritis severity clinical scores compared to that of vehicle-treated rats with PIA, with no differences observed between rats treated with the different doses of IbTX tested (Fig. 3A). In comparison, rats with PIA treated with 2 mg/kg paxilline exhibited only a slight reduction in disease severity, whereas those treated with 20 mg/kg paxilline exhibited a greater than 50% reduction in disease severity (Fig. 3B), similar to IbTX and in agreement with our previous findings (Tanner et al., 2015).Hematoxylin & eosin staining and safranin O/fast green staining of joint sections indicate that rats with PIA treated with 0.5 mg/kg IbTX had fewer immune infiltrates, pannus extensions, synovial hyperplasia, and cartilage erosions compared to vehicle-treated animals (Fig. 3C and D), while X-rays indicate that PIA rats treated with 0.5 mg/kg IbTX had significantly reduced bone damage compared to vehicle-treated rats (Fig. 3E). FLS isolated from 0.5 mg/kg IbTX-treated PIA rats and cultured for at least three passages were significantly less invasive compared to FLS isolated from vehicle-treated PIA rats and cultured for the same duration (Fig. 3F). Their invasiveness was comparable to that of FLS from healthy rats.

In order to determine the efficacy of IbTX in rats that had already developed severe paw inflammation, mimicking the RA patient with established disease, rats with PIA were treated with 0.5 mg/kg IbTX or vehicle seven days after they first exhibited signs of disease, at which point paw inflammation was already severe. PIA rats treated with IbTX every other day showed a significant decrease in paw inflammation after a 3-4 day lag time, whereas inflammation in vehicle-treated rats remained severe (Fig. 4A). In order to determine how long IbTX remains effective after cessation of treatment, rats with PIA were treated with 0.5 mg/kg IbTX for only the first 7 days following disease onset. IbTX-treated rats had significantly decreased paw inflammation on days 6 and 7 after the start

of treatment; however, disease severity returned to levels comparable to vehicle after stopping treatment within 2-3 days (Fig. 4B).

To further verify the efficacy of IbTX *in vivo*, we tested it in the CIA model of RA. Rats with CIA were treated with either vehicle or 0.5 mg/kg IbTX every other day starting at disease onset. Similar to results in PIA, rats treated with IbTX had significantly less joint swelling compared to vehicle-treated rats (Fig. 5A). CIA-FLS isolated from IbTX-treated rats and cultured for at least three passages were less invasive than CIA-FLS isolated from vehicle-treated rats and cultured for the same duration (Fig. 5B) and X-rays and histology of paws indicate less bone damage, as well as fewer immune infiltrates, pannus extensions, synovial hyperplasia, and cartilage erosions in IbTX-treated animals compared to those treated with vehicle (Fig. 5C-E).

Paxilline, but not IbTX, induces tremors in rats

KCa1.1 channels composed of the α and β4 subunit are found in the CNS and loss of neuronal KCa1.1 expression or function causes tremors (Imlach et al., 2008; Wang et al., 2014). We therefore tested whether paxilline and IbTX induce tremors in rats. We chose doses of the blockers, 20 mg/kg paxilline and 0.5 mg/kg IbTX, which showed similar efficacy in the PIA and CIA models of RA in terms of clinical signs, joint inflammation, and cartilage degradation (Fig. 3 and 5) (Tanner et al., 2015). Vehicle-treated rats exhibited no tremors (Fig. 6A). Paxilline-treated rats exhibited abrupt events of increased acceleration (Fig. 6B), indicating the presence of tremor events. IbTX-treated rats exhibited no tremors and displayed acceleration measurements comparable to that of vehicle-treated rats (Fig. 6C). By setting a threshold of 0.15 m/s^2 above the root-mean-

square (RMS) transformed data (Fig. 6D-F) and counting the number of events the RMS-transformed acceleration passed above this threshold, we determined that paxilline-treated rats had approximately 14 ± 4 tremor events during the recordings 10 minutes after treatment (Fig. 6G). Tremor frequency decreased over time. In sharp contrast, vehicle and IbTX-treated rats exhibited no tremors (Fig. 6G). Quantifying tremors through the integral of the RMS-transformed acceleration determined that paxilline-treated rats had high intensity tremors soon after treatment, which decreased over time, while vehicle and IbTX-treated rats did not exhibit such changes in acceleration intensity (Fig. 6H). Taken together, these data indicate that paxilline, but not IbTX, induces tremors in rats.

Paxilline, but not IbTX, induces incontinence in rats

Considering that IbTX and paxilline both block KCa1.1 channels associated with the β1 subunit that is found in smooth muscle, including that of the urinary bladder (Poulsen et al., 2009), we tested whether they cause incontinence in rats. Healthy Lewis rats were treated with either vehicle, paxilline, or IbTX. An hour later, paxilline-treated rats exhibited a large number of urine spots, indicating a lack of bladder control. Surprisingly, IbTX-treated animals exhibited a similar small number of urine spots as vehicle-treated rats (Fig. 7). This indicates that IbTX does not induce incontinence, while paxilline does.

Discussion

In this study, we validated the peptide KCa1.1 blocker IbTX for efficacy in reducing the *ex vivo* invasiveness of FLS from patients with RA and from multiple rat models of RA. We also show that IbTX reduces disease severity in both the PIA and CIA rat models

of RA, while not inducing tremors or incontinence. Together, these data suggest IbTX as a potential novel therapeutic for RA by inhibiting FLS and without inducing side effects seen with broad KCa1.1 blockade.

No animal model of RA fully recapitulates all aspects of the human disease; we therefore assayed IbTX for efficacy in both the PIA and CIA, two well-established models of RA in rats. Though IbTX significantly reduced disease severity in both models to a similar degree as paxilline (Tanner et al., 2015), IbTX-treated animals still exhibited a significant amount of paw inflammation. The inability of KCa1.1 blockers to eliminate inflammation may be due to other cell-types involved in RA such as T lymphocytes, chondrocytes, and osteoclasts, which may still have pathogenic phenotypes following IbTX treatment (Lundy et al., 2007; Otero and Goldring, 2007; Schett, 2007). IbTX likely does not have an effect on T lymphocytes in RA as these cells express different potassium channels from KCa1.1, which are insensitive to IbTX and paxilline (Beeton and Chandy, 2005; Beeton et al., 2011). Osteoclasts and chondrocytes express several potassium channels, including KCa1.1 (Arkett et al., 1994; Mobasheri et al., 2012; Weidema et al., 2000). The regulatory β subunits of KCa1.1 expressed by these cells and if IbTX has an effect on their destructive functions during RA have yet to be investigated. It is possible that a combined therapy consisting of inhibitors specific for each of these cell-types will be needed to further reduce disease severity in models of RA. Alternatively, it may be possible for a combined treatment of IbTX with a currently available RA therapy, such as a TNF-α antagonist, to have an additive effect at treating RA by using IbTX to target FLS and a currently available therapy to reduce inflammation.

We examined the effect of KCa1.1 blockers on the *in vitro* invasion of FLS that were passaged multiple times. From this, we infer that KCa1.1 blockers reduce disease severity in rat models of RA at least in part from reducing FLS invasion *in vivo.* Passaging these cells is a standard practice to isolate FLS and is necessary to obtain a population solely composed of FLS without any contaminating macrophage-like synoviocytes, synovial-infiltrating immune cells, or endothelial cells that either die or are washed away through multiple *in vitro* passages (Bartok and Firestein, 2010; Rosengren et al., 2007). Passaged RA-FLS and PIA-FLS maintain a high level of invasiveness and secrete pro-inflammatory cytokines and proteases following passaging, indicating that passaged FLS maintain a pathogenic phenotype *in vitro* (Bartok and Firestein, 2010; Laragione et al., 2008; Tanner et al., 2015). The *in vitro* invasion of passaged FLS is also directly correlated with radiographic damage in patients with RA, as well as in PIA (Laragione et al., 2008; Tolboom et al., 2005). Furthermore, our data indicate that FLS in the synovium *in situ* of rats with CIA express KCa1.1 with the β3 subunit, supporting the notion that FLS maintain similar potassium channel phenotypes *in vivo* and *in vitro*. Therefore, it is likely that the potassium channel phenotype of FLS and effects of KCa1.1 blockers on FLS phenotypes are similar *in vitro* and *in vivo*.

PIA rats treated with IbTX for only the first week after disease onset exhibited a rapid increase in joint swelling once treatment ceased, indicating that IbTX was only efficacious with continuous administration. This may be due to proteolytic degradation of the peptide *in vivo*. Alternatively, as IbTX has a molecular weight of only 4.231 kDa, below the cutoff of 30-50 kDa for glomerular filtration, it could be rapidly eliminated by renal clearance. The addition of polyethylene glycol (PEG) moieties is a widely used method to increase

the length of efficacy of therapeutics by reducing renal clearance and decreasing the rate of proteolytic degradation (Harris and Chess, 2003; Turecek et al., 2016). Creating a PEGylated IbTX analog could therefore be used to increase its length of efficacy. Indeed, such an approach has successfully been used to improve the duration of efficacy of other venom-derived peptide potassium channel blockers (Tanner et al., 2017b).

In this study we used a smart phone's accelerometer to measure tremors in rats. Other techniques used to measure tremors in laboratory settings involve the use of electrodes implanted into the back muscles of rats and measuring contractions over time (Feketa et al., 2013). Such techniques involve the use of specialized equipment and software, as well as survival surgeries that are stressful for the animals. Our technique using a smart phone's accelerometer is non-invasive and minimally stressful for the rats, as it requires no surgery, and is more cost-effective compared to surgical interventions. In addition, this technique was effective at quantifying the tremors observed in paxilline-treated rats and at differentiating the presence and absence of tremors, making it a valuable technique to quickly screen whether potential drugs are tremorigenic *in vivo*. Similar accelerometer-based technologies have also been used to observe tremors in rats and mice (Miyazaki et al., 2014; Shih and Young, 2007) and smart phone-based accelerometry apps have even been used to monitor tremors in patients with Parkinson's disease (Joundi et al., 2011; Kostikis et al., 2015).

Paxilline given intraperitoneally at 20 mg/kg every-other-day reduces signs of disease in rat models of RA, whereas 2 mg/kg given at the same frequency had only minimal improvement in clinical signs of disease (Tanner et al., 2015). IbTX at doses of 0.05-5 mg/kg subcutaneously every-other-day, gave a similar efficacy as paxilline in treating CIA

and PIA. This discrepancy in dosing efficacy was due to venom-derived potassium channel blocking peptides creating a depot under the skin when given subcutaneously and entering the circulation over hours (Tarcha et al., 2012). This allows for small doses to provide sustained benefit, as opposed to giving a bolus of paxilline intraperitoneally with a half-life of less than one hour (Tanner et al., 2015).

Paxilline is a well-known tremorgenic compound as it is a lipophilic small molecule that can cross membranes to enter the CNS and other tissues and blocks KCa1.1 channels regardless of β subunit expression (Imlach et al., 2008). For these reasons, we also expected that paxilline would induce incontinence (Meredith et al., 2004). The lack of tremor induction by IbTX was anticipated as this peptide blocks KCa1.1 only in the absence of β4 subunits and these subunits are widely expressed in the CNS. The lack of incontinence in rats treated with IbTX was surprising as this is induced by the targeting of KCa1.1 expressed by smooth muscle cells in the urinary bladder. These cells express the β1 subunit of KCa1.1 and IbTX blocks KCa1.1 containing this subunit. However, smooth muscle cells are separated from the circulation by endothelial cells and from the urine by bladder epithelial cells. IbTX is likely unable to cross these barriers and therefore unable to reach the smooth muscle cell KCa1.1 channels.

Our studies of potential side effects associated with blocking KCa1.1 focused on tremors and incontinence. However, due to the tissue distribution of this channel, there may be other side effects from blocking KCa1.1. These include hypertension, as KCa1.1 associated with the β1 subunit is found in the smooth muscle of blood vessels in rats (Brenner et al., 2000; Poulsen et al., 2009). Though, given our results indicating a lack of effect of IbTX on the urinary bladder it is likely that IbTX also does not affect vascular

smooth muscle, which is separated from the circulation by a layer of endothelium that IbTX may not be able to cross. Male fertility may also be affected, as KCa1.1 associated with the β3 subunit is found in the rat testis and human spermatozoa (Mannowetz et al., 2013; Poulsen et al., 2009). However, IbTX may not be able to cross through the blood-testis barrier. Furthermore, KCa1.1 associated with the β2 subunit is found in the human pancreas and kidney and blocking this channel may have detrimental effects on these tissues as well (Uebele et al., 2000). In order to more completely validate IbTX as a therapeutic for use in humans, these side effects associated with KCa1.1 block in these tissues will need to be examined. It is indeed possible that IbTX, as well as paxilline, will induce side effects from affecting these tissues, as IbTX can block KCa1.1 associated with subunits β1-3 or with no β subunits. If this is the case, it may be necessary to identify any unique splice variants of KCa1.1 pore-forming α subunits expressed by FLS and generate a KCa1.1 blocker specific for this unique aspect, along with the β3 subunit, of the channel in order to create a more viable therapeutic for RA. Regardless, our findings that IbTX does not induce tremors or incontinence show that selectively inhibiting KCa1.1 in a β subunit-specific manner can be a viable means of treating diseases mediated by this potassium channel without inhibiting all variants of this channel.

Overall, this study indicates the KCa1.1 potassium channel blocker IbTX as an inhibitor of the invasive phenotype of FLS and that IbTX reduces disease severity in two rat models of RA. We have also shown that KCa1.1 block with IbTX eliminates two major side effects observed during systemic KCa1.1 blockade with small molecules and in mice lacking KCa1.1 α expression (Imlach et al., 2008; Meredith et al., 2004). Taken together, these data indicate IbTX as either a potential novel therapeutic for the treatment of RA by

targeting KCa1.1 channels expressed on FLS or as a scaffold for the future generation of RA-FLS selective KCa1.1 blockers.

Acknowledgements

We would like to thank Dr. Sean Marrelli (Department of Anesthesiology, Baylor College of Medicine) for assisting us with the calculations and data analysis of tremor measurements. We acknowledge excellent service from the Mouse Metabolism and Phenotyping and Pathology and Histology Cores at Baylor College of Medicine.

Authorship Contributions

Participated in research design: M.R.T., C.B.

Conducted experiments: M.R.T., B.H.C., R.H., E.J.G., C.B.

Contributed new reagents or analytic tools: M.W.P., T.L., P.S.G.

Performed data analysis: M.R.T., C.B.

Wrote or contributed to the writing of the manuscript: M.R.T., M.W.P., B.H.C., R.H., E.J.G., T.L., P.S.G., C.B.

References

Aletaha D, Neogi T, Silman A, Funovits J, Felson D, Bingham C, Birnbaum N, Burmester G, Bykerk V, Cohen M, Combe B, Costenbader K, Dougados M, Emery P, Ferraccioli G, Hazes J, Hobbs K, Huizinga T, Kavanaugh A, Kay J, Kvien T, Laing T, Mease P, Ménard H, Moreland L, Naden R, Pincus T, Smolen J, Stanislawska-Biernat E, Symmons D, Tak P, Upchurch K, Vencovský J, Wolfe F and Hawker G (2010) 2010 Rheumatoid arthritis classification criteria: an American College of Rheumatology/European League Against Rheumatism collaborative initiative. *Arthritis Rheum* **62**.

Arkett S, Dixon J, Yang J, Sakai D, Minkin C and Sims S (1994) Mammalian osteoclasts express a transient potassium channel with properties of Kv1.3. *Receptors Channels* **2**:281-293.

Bartok B and Firestein G (2010) Fibroblast-like synoviocytes: key effector cells in rheumatoid arthritis. *Immunol Rev* **233**:233-255.

Beeton C (2017) KCa1.1 chanenls as therapeutic targets for rheumatoid arthritis. *Expert Opin Ther Targets* **21**:1077-1081.

Beeton C and Chandy K (2005) Potassium channels, memory T cells, and multiple sclerosis. *Neuroscientist* **11**:550-562.

Beeton C, Pennington M and Norton R (2011) Analogs of the sea anemone potassium channel blocker ShK for the treatment of autoimmune diseases. *Inflamm Allergy Drug Targets* **10**:313-321.

Beeton C, Wulff H, Standifer N, Azam P, Mullen K, Pennington M, Kolski-Andreaco A, Wei E, Grino A, Counts D, Wang P, LeeHealey C, S Andrews B, Sankaranarayanan A, Homerick D, Roeck W, Tehranzadeh J, Stanhope K, Zimin P, Havel P, Griffey S, Knaus H, Nepom G, Gutman G, Calabresi P and Chandy K (2006) Kv1.3 channels are a therapeutic target for T cell-mediated autoimmune diseases. *Proc Natl Acad Sci USA* **103**:17414-17419.

Bottini N and Firestein G (2013) Duality of fibroblast-like synoviocytes in RA: passive responders and imprinted aggressors. *Nat Rev Rheumatol* **9**:24-33.

Brenner M, Meng H, Yarlett N, Griffiths M, Remmers E, Wilder R and Gulko P (2005) The non-major histocompatibility complex quantitative trait locus Cia10 contains a major arthritis gene and regulates disease severity, pannus formation, and joint damag. *Arthritis Rheum* **52**:322-332.

Brenner R, Peréz G, Bonev A, Eckman D, Kosek J, Wiler S, Patterson A, Nelson M and Aldrich R (2000) Vasoregulation by the beta1 subunit of the calcium-activated potassium channel. *Nature* **407**:870-876.

Feketa V, Balasubramanian A, Flores C, Player M and Marrelli S (2013) Shivering and tachycardic responses to external cooling in mice are substantially suppressed by TRPV1 activation but not by TRPM8 inhibition. *Am J Physiol Regul Integr Comp Physiol* **305**:R1040-R1050.

Galvez A, Gimenez-Gallego G, Reuben J, Roy-Contancin L, Feigenbaum P, Kaczorowski G and Garcia M (1990) Purification and characterization of a unique, potent, peptidyl probe for the high conductance calcium-activated potassium channel from venom of the scorpion Buthus tamulus. *J Biol Chem* **265**:11083-11090.

Griffiths M, Cremer M, Harper D, McCall S and Cannon G (1992) Immunogenetics of collagen-induced arthritis in rats. Both MHC and non-MHC gene products determine the epitope specificity of immune response to bovine and chick type II collagens. *J Immunol* **149**:309-316.

Harris J and Chess R (2003) Effect of pegylation on pharmaceuticals. *Nat Rev Drug Discov* **2**(214-221).

Helmick C, Felson D, Lawrence R, Gabriel S, Hirsch R, Kwoh C, Liang M, Kremers H, Mayes M, Merkel P, Pillemer S, Reveille J, Stone J and Workgroup NAD (2008) Estimates of the prevalence of arthritis and other rheumatic conditions in the United States. Part I. *Arthritis Rheum* **58**:15-25.

Hu X, Laragione T, Sun L, Koshy S, Jones K, Ismailov I, Yotnda P, Horrigan F, Gulko P and Beeton C (2012) KCa1.1 potassium channels regulate key proinflammatory and invasive

properties of fibroblast-like synoviocytes in rheumatoid arthritis. *J Biol Chem* **287**:4014-4022.

Imlach W, Finch S, Dunlop J, Meredith A, Aldrich R and Dalziel J (2008) The molecular mechanism of "ryegrass staggers," a neurological disorder of K+ channels. *J Pharmacol Exp Ther* **327**:657-664.

Joundi R, Brittain J, Jenkinson N, Green A and Aziz T (2011) Rapid tremor frequency assessment with the iPhone accelerometer. *Parkinsonism Relat Disord* **17**:288-290.

Kahlenberg J and Fox D (2011) Advances in the medical treatment of rheumatoid arthritis. *Hand Clin* **27**:11-20.

Kostikis N, Hristu-Varsakelis D, Arnaoutoglou M and Kotsavasiloglou C (2015) A smartphone-based tool for assessing parkinsonian hand tremor. *IEEE J Biomed Health Inform* **19**:1835-1842.

Laragione T, Brenner M, Mello A, Symons M and Gulko P (2008) The arthritis severity locus Cia5d is a novel genetic regulator of the invasive properties of synovial fibroblasts. *Arthritis Rheum* **58**:2296-2306.

Laragione T and Gulko P (2010) mTOR regulates the invasive properties of synovial fibroblasts in rheumatoid arthritis. *Mol Med* **16**:352-258.

Li W, Gao S, Lv C, Wu Y, Guo Z, Ding J and Xu T (2007) Characterization of voltage-and Ca2+-activated K+ channels in rat dorsal root ganglion neurons. *J Cell Physiol* **212**:348-357.

Lippiat J, Standen D, Harrow I, Phillips S and Davies N (2003) Properties of BK(Ca) channels formed by bicistronic expression of hSloalpha and beta1-4 subunits in HEK293 cells. *J Membr Biol* **192**:141-148.

Löhn M, Lauterbach B, Haller H, Pongs O, Luft F and Gollasch M (2001) beta(1)-Subunit of BK channels regulates arterial wall[Ca(2+)] and diameter in mouse cerebral arteries. *J Appl Physiol* **91**:1350-1354.

Lundy S, Sarkar S, Tesmer L and Fox D (2007) Cells of the synovium in rheumatoid arthritis. T lymphocytes. *Arthritis Res Ther* **9**:202.

Mannowetz N, Naidoo N, Choo S, Smith J and Lishko P (2013) Slo1 is the principal potassium channel of human spermatozoa. *Elife* **2**:e01009.

Meera P, Wallner M and Toro L (2000) A neuronal beta subunit (KCNMB4) makes the large conductance, voltage- and Ca2+-activated K+ channel resistant to charybdotoxin and iberiotoxin. *Proc Natl Acad Sci USA* **97**:5562-5567.

Meredith A, Thorneloe K, Werner M, Nelson M and Aldrich R (2004) Overactive bladder and incontinence in the absence of the BK large conductance Ca2+-activated K+ channel. *J Biol Chem* **279**:36746-36752.

Miyazaki H, Oyama F, Inoue R, Aosaki T, Abe T, Kiyonari H, Kino Y, Kurosawa M, Shimizu J, Ogiwara I, Yamakawa K, Koshimizu Y, Fujiyama F, Kaneko T, Shimizu H, Nagatomo K, Yamada K, Shimogori T, Hattori N, Miura M and Nukina N (2014) Singular localization of sodium channel β4 subunit in unmyelinated fibres and its role in the striatum. *Nat Commun*:5525.

Mobasheri A, Lewis R, Ferreira-Mendes A, Rufino A, Dart C and Barrett-Jolley R (2012) Potassium channels in articular chondrocytes. *Channels (Austin)* **6**:416-425.

Otero M and Goldring M (2007) Cells of the synovium in rheumatoid arthritis. Chondrocytes. *Arthritis Res Ther* **9**:220.

Pethő Z, Tanner M, Tajhya R, Huq R, Laragione T, Panyi G, Gulko P and Beeton C (2016) Different expression of β subunits of the KCa1.1 channel by invasive and non-invasive human fibroblast-like synoviocytes. *Arthritis Res Ther* **18**:103.

Poulsen A, Wulf H, Hay-Schmidt A, Jansen-Olesen I, Olesen J and Klaerke D (2009) Differential expression of BK channel isoforms and beta-subunits in rat neuro-vascular tissues. *Biochim Biophys Acta* **1788**:380-389.

Rosengren S, Boyle D and Firestein G (2007) Acquisition, culture, and phenotyping of synovial fibroblasts. *Methods Mol Med* **135**:365-375.

Sanchez M and McManus O (1996) Paxilline Inhibition of the Alpha-Subunit of the High-Conductance Calcium-Activated Potassium Channel. *Neuropharmacology* **35**:963-968.

Schett G (2007) Cells of the synovium in rheumatoid arthritis. Osteoclasts. *Arthritis Res Ther* **9**:203.

Shih Y and Young M (2007) Integrated digital image and accelerometer measurements of rat locomotor and vibratory behaviour. *J Neurosci Methods* **166**:81-88.

Tajhya R, Hu X, Tanner M, Huq R, Kongchan N, Neilson J, Rodney G, Horrigan F, Timchenko L and Beeton C (2016) Functional KCa1.1 channels are crucial for regulating the proliferation, migration and differentiation of human primary skeletal myoblasts. *Cell Death Dis* **7**:e2426.

Tanner M and Beeton C (2018) Differences in ion channel phenotype and function between humans and animal models. *Front Biosci* **23**:43-64.

Tanner M, Hu X, Tajhya R, Sun L, Khan F, Laragione T, Horrigan F, Gulko P and Beeton C (2015) KCa1.1 inhibition attenuates fibroblast-like synoviocyte invasiveness and ameliorates disease in rat models of rheumatoid arthritis. *Arthritis Rheumatol* **67**:96-106.

Tanner M, Pennington M, Laragione T, Gulko P and Beeton C (2017a) KCa1.1 channels regulate β1 integrin function and cell adhesion in rheumatoid arthritis fibroblast-like synoviocytes. *FASEB J* **31**:3309-3320.

Tanner M, Tajhya R, Huq R, Gehrmann E, Rodarte K, Atik M, Norton R, Pennington M and Beeton C (2017b) Prolonged immunomodulation in inflammatory arthritis using the selective Kv1.3 channel blocker HsTX1[R14A] and its PEGylated analog. *Clin Immunol* **180**:45-57.

Tarcha E, Chi V, Muñoz-Elías E, Bailey D, Londono L, Upadhyay S, Norton K, Banks A, Tjong I, Nguyen H, Hu X, Ruppert G, Boley S, Slauter R, Sams J, Knapp B, Kentala D, Hansen Z, Pennington M, Beeton C, Chandy K and Iadonato S (2012) Durable pharmacological

responses from the peptide ShK-186, a specific Kv1.3 channel inhibitor that suppresses T cell mediators of autoimmune disease. *J Pharmacol Exp Ther*:642-653.

Tauc M, Congar P, Poncet V, Merot J, Vita C and Poujeol P (1993) Toxin pharmacology of the large-conductance Ca(2+)-activated K+ channel in the apical membrane of rabbit proximal convoluted tubule in primary culture. *Pflugers Arch* **425**:126-133.

Tolboom T, van der Helm-Van Mil A, Nelissen R, Breedveld F, Toes R and Huizinga T (2005) Invasiveness of fibroblast-like synoviocytes is an individual patient characteristic associated with the rate of joint destruction in patients with rheumatoid arthritis. *Arthritis Rheum* **52**:1999-2002.

Turecek P, Bossard M, Schoetens F and Ivens I (2016) PEGylation of biopharmaceuticals: a review of chemistry and nonclinical safety information of approved drugs. *J Pharm Sci* **105**:460-475.

Uebele V, Lagrutta A, Wade T, Figueroa D, Liu Y, McKenna E, Austin C, Bennett P and Swanson R (2000) Cloning and Functional Expression of Two Families of β-Subunits of the Large Conductance Calcium-activated K+ Channel. *J Biol Chem* **275**:23211-23218.

Wang B, Jaffe D and Brenner R (2014) Current understanding of iberiotoxin-resistant BK channels in the nervous system. *Front Physiol* **5**:382.

Weidema A, Dixon S and Sims S (2000) Electrophysiological characterization of ion channels in osteoclasts isolated from human deciduous teeth. *Bone* **27**:5-11.

Yu M, Liu S, Sun P, Pan H, Tian C and Zhang L (2016) Peptide toxins and small-molecule blockers of BK channels. *Acta Pharmacol Sin* **37**:56-66.

Footnotes

This work was supported by the Arthritis Foundation [Grant 6483] and the National Institutes of Health [Grants GM088129, AI050831, AR069960, HL007676, CA125123, and HG006348].

Figure legends

Fig. 1. KCa1.1 is expressed on CIA-FLS *in vivo*. A-C, Example images of synovial tissue from rats with CIA that had signs of disease for 14 days stained for expression of KCa1.1α (red) and KCa1.1β3 (brown) (Panel A), the FLS marker podoplanin (red) and KCa1.1α (brown) (Panel B), or the FLS marker cadherin-11 (red) and KCa1.1α (brown) (Panel C). Images are at 40x (Left) or 80x magnification (Right) and dashed boxes on the left panels demarcate the areas magnified to 80x shown on the right. Scale bars = 50 μm.

Fig. 2. IbTX inhibits KCa1.1 channels expressed on FLS and reduces *ex vivo* FLS invasion. A, Representative whole-cell potassium currents (top) in RA-FLS, PIA-FLS, and CIA-FLS before (grey) and after administration of 3 nM IbTX (black) and dose-response inhibition of potassium currents by IbTX (bottom). B, Invasiveness of FLS from patients with RA and rats with either PIA or CIA through Matrigel-coated Transwell inserts in the presence of 10 μM paxilline (Pax) or 10 μM IbTX. Mean ± SEM. N=3 donors per group. *p<0.05, **p<0.01, ***p<0.001.

Fig. 3. IbTX reduces signs of disease in PIA. A, Clinical scores of paw inflammation from rats with PIA treated with vehicle (white) or 0.05 mg/kg (red), 0.5 mg/kg (grey), or 5 mg/kg IbTX (blue) subcutaneously every-other-day starting at disease onset. Mean ± SEM. N=6 rats in the 0.05 mg/kg IbTX and 5 mg/kg IbTX groups, N=9 rats in the 0.5 mg/kg IbTX group, N=15 rats in the vehicle-treatment group. B, Clinical scores of paw inflammation from rats with PIA treated with vehicle (white), 2 mg/kg paxilline (black), or 20 mg/kg paxilline (green) intraperitoneally every-other-day starting at disease onset, N=7-8 rats

per group. C, Hematoxylin & eosin staining (top) and safranin O/fast green staining (bottom) of tissue sections of paws from rats with PIA treated with vehicle (left) or IbTX (right). Arrows indicate areas of hyperplasia (hematoxylin & eosin) and cartilage erosions (safranin O/fast green). Scale bars = 100 μm. D, Histology scoring of paw joints of rats with PIA treated with vehicle (white) or 0.5 mg/kg IbTX (grey). Mean ± SEM. N=4 paws per group. E, Example x-rays of hind paws from vehicle (left) and IbTX-treated (right) rats. F, *Ex vivo* invasion of FLS isolated from 3 healthy DA rats, 3 rats with PIA treated with vehicle, and 3 rats with PIA treated with 0.5 mg/kg IbTX through Matrigel-coated Transwell inserts. Mean ± SEM. N=3 per group. *p<0.05, ***p<0.001.

Fig. 4. A, Clinical scores of paw inflammation from rats with PIA treated with vehicle (black) or with 0.5 mg/kg IbTX (grey) every-other-day starting 7 days after disease onset. Mean ± SEM. N=5-6 rats per group. B, Clinical scores of rats with PIA treated with vehicle (black) or with IbTX (grey) every-other-day for the first 7 days following disease onset. Mean ± SEM. N=6 rats per group. *p<0.05, **p<0.01.

Fig. 5. IbTX reduces disease severity in the CIA rat model of RA. A, Clinical scores of paw inflammation of rats with CIA treated with vehicle (black) or 0.5 mg/kg IbTX (grey) every-other-day starting at disease onset. Mean ± SEM. N=12 rats per group. B, *Ex vivo* invasiveness of FLS from 3 healthy Lewis rats, 3 rats with CIA treated with vehicle, and 3 rats with CIA treated with 0.5 mg/kg IbTX through Matrigel-coated Transwell inserts. Mean ± SEM. N=3 per group. C, Example X-ray images of paws from rats with CIA treated every-other-day with vehicle (left) or IbTX (right) for 14 days after disease onset. D,

Hematoxylin & eosin staining (top) and safranin-O/fast green staining (bottom) of tissue sections of paws from rats with CIA treated with vehicle (left) or IbTX-treated (right). Arrows indicate areas of hyperplasia (hematoxylin & eosin) and cartilage erosions (safranin O/fast green). Scale bars = 100 μm. E, Histology scoring of paw joints of rats with CIA treated with vehicle (white) or IbTX (grey). Mean ± SEM. N=3 paws per group. *p<0.05, **p<0.01.

Fig. 6. Paxilline, but not IbTX, causes tremors in rats. A-C, Example acceleration recordings of rats treated with vehicle (A), 20 mg/kg paxilline (Pax) (B), or 0.5 mg/kg IbTX (IbTX) (C). D-F, root-mean-square (RMS) transformed accelerations from the raw data presented in A-C. Red lines indicate the threshold above background acceleration. G, Numbers of tremor events above the threshold of the RMS-transformed acceleration of rats treated with vehicle, paxilline, or IbTX 10 minutes, 1 hour, and 24 hours after treatment. Mean ± SEM. N=6 rats per group. H, Tremor intensity of rats treated with vehicle, paxilline, or IbTX 10 minutes, 1 hour, and 24 hours after treatment. Mean ± SEM. N=6 rats per group. *p<0.05, **p<0.01 when compared to the vehicle-treated group.

Fig. 7. Paxilline, but not IbTX, induces incontinence in rats. The number of urine spots counted from healthy Lewis rats treated with either vehicle, 20 mg/kg paxilline (Pax), or 0.5 mg/kg IbTX, and then given an oral gavage of water and placed individually in a paper towel-lined cage for one hour. Mean ± SEM. N=6 rats per group. **p<0.01 when compared to the vehicle-treated group.

JPET Fast Forward. Published on February 16, 2018 as DOI: 10.1124/jpet.117.245118
This article has not been copyedited and formatted. The final version may differ from this version.

Figure 1

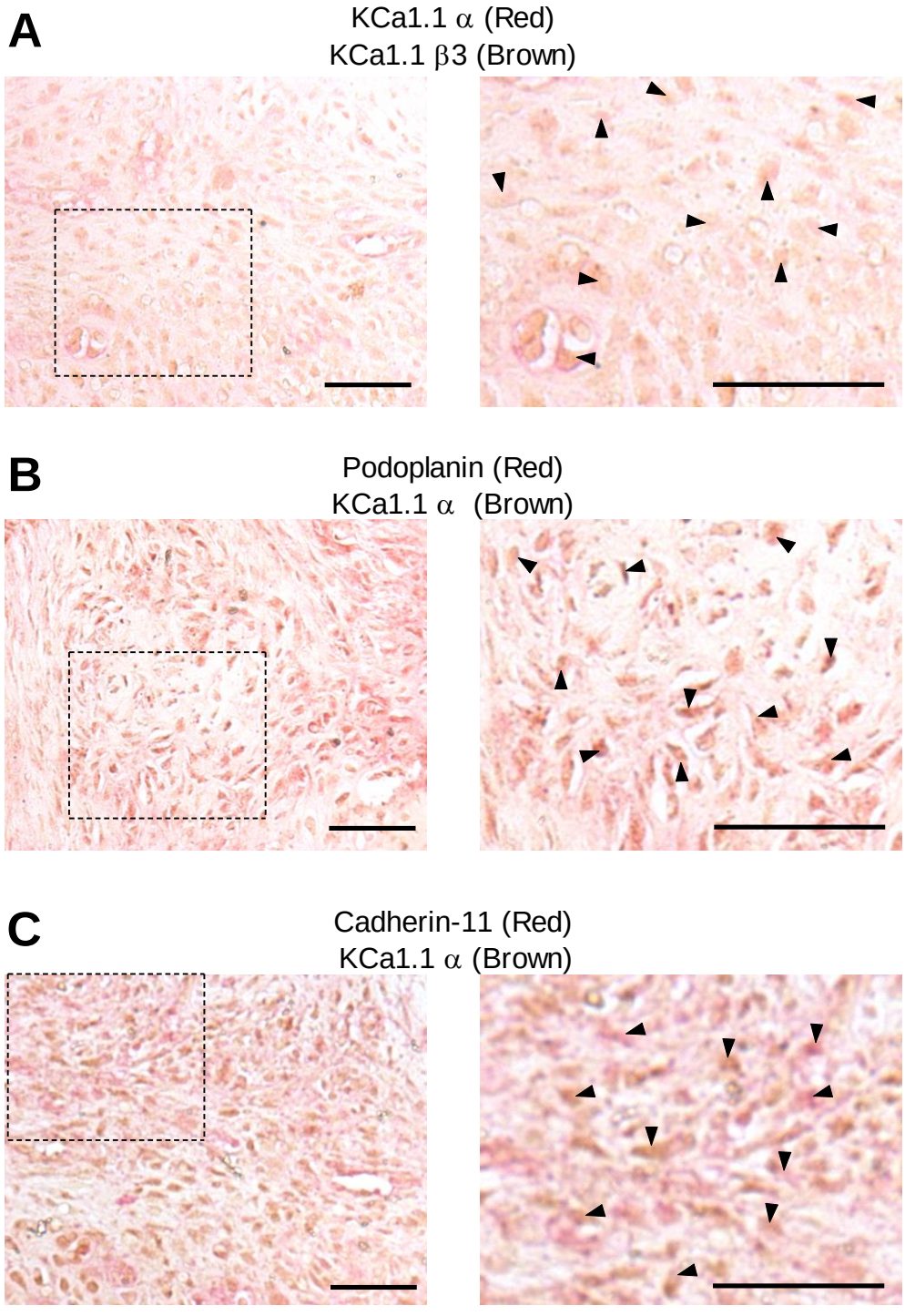

JPET Fast Forward. Published on February 16, 2018 as DOI: 10.1124/jpet.117.245118
This article has not been copyedited and formatted. The final version may differ from this version.

Figure 2

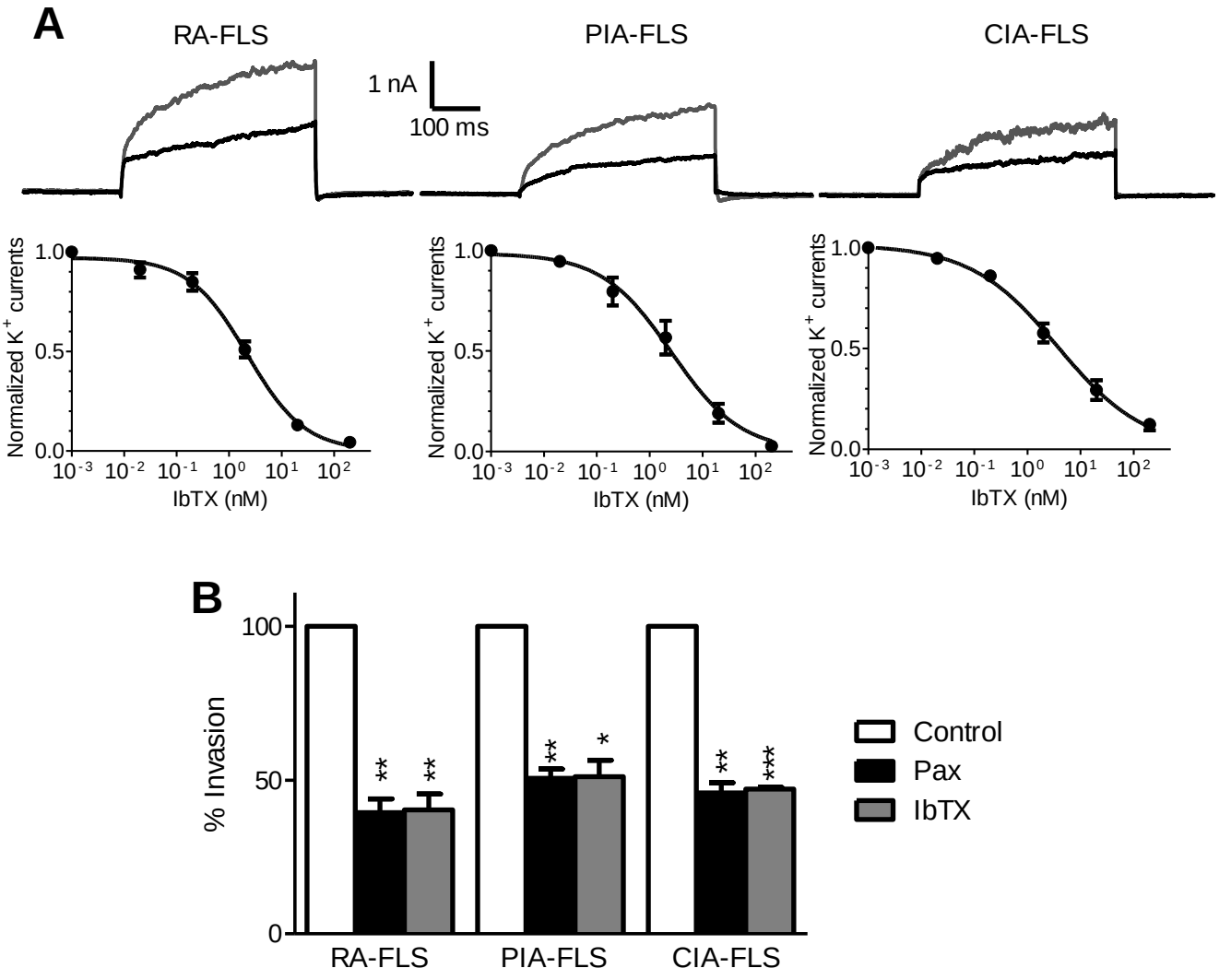

JPET Fast Forward. Published on February 16, 2018 as DOI: 10.1124/jpet.117.245118
This article has not been copyedited and formatted. The final version may differ from this version.

Figure 3

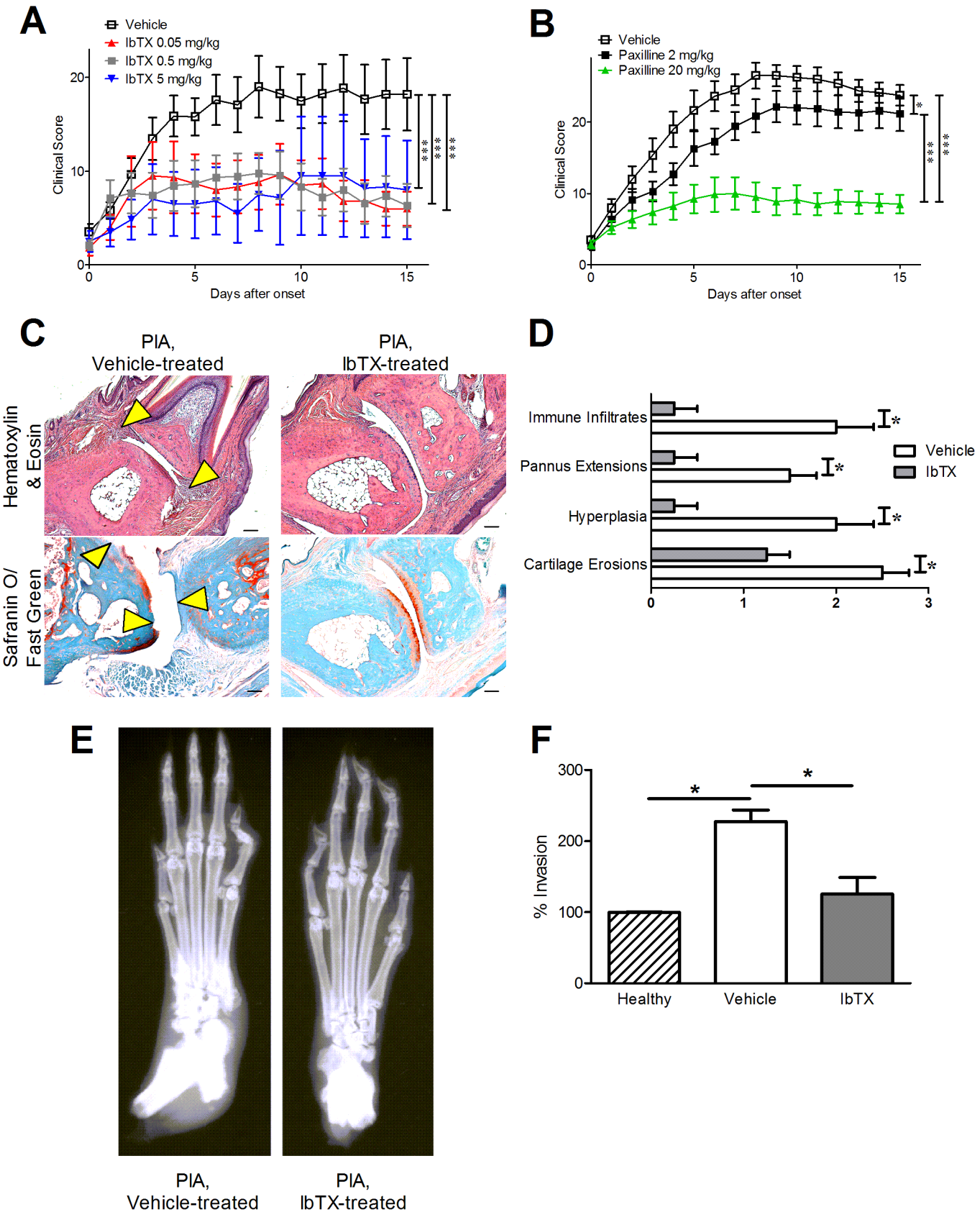

JPET Fast Forward. Published on February 16, 2018 as DOI: 10.1124/jpet.117.245118
This article has not been copyedited and formatted. The final version may differ from this version.

Figure 4

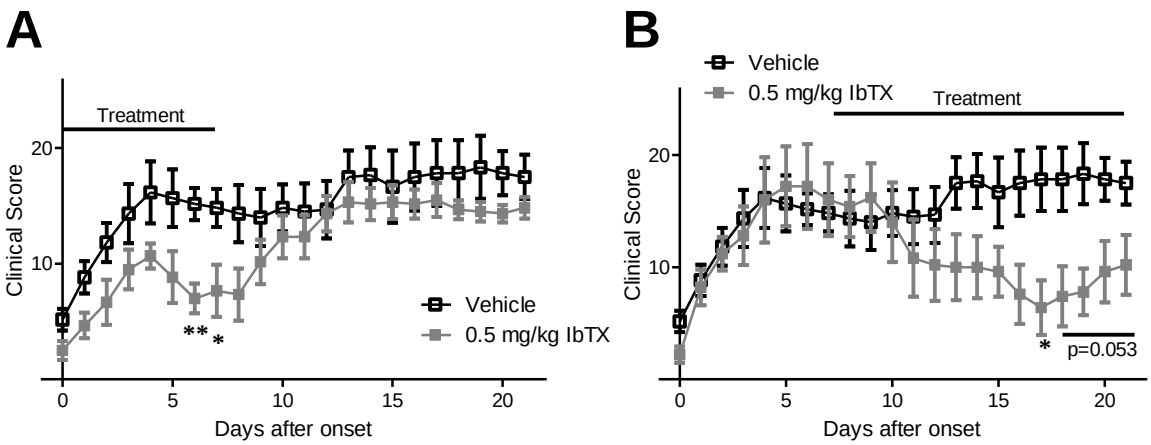

JPET Fast Forward. Published on February 16, 2018 as DOI: 10.1124/jpet.117.245118
This article has not been copyedited and formatted. The final version may differ from this version.

Figure 5

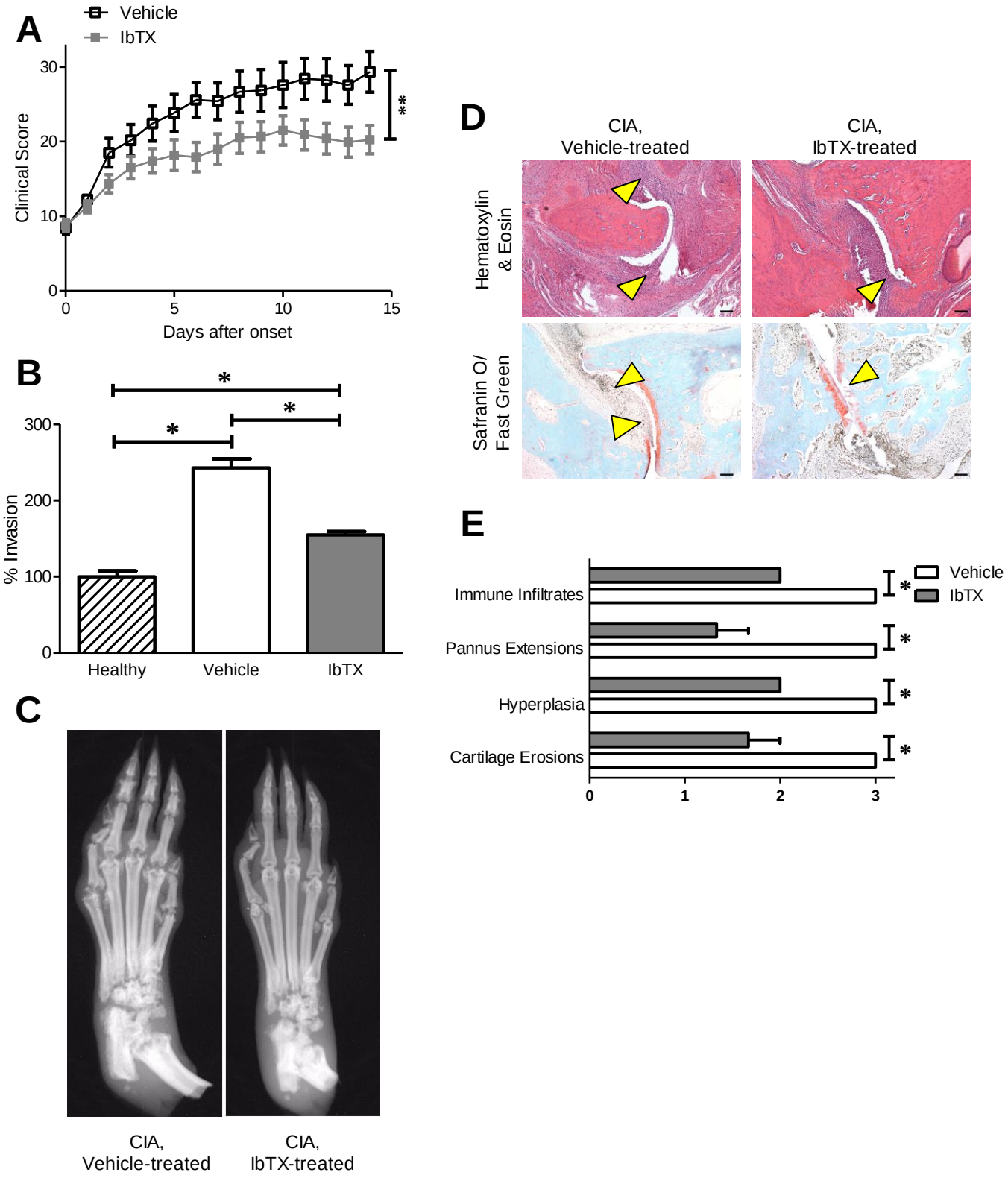

JPET Fast Forward. Published on February 16, 2018 as DOI: 10.1124/jpet.117.245118
This article has not been copyedited and formatted. The final version may differ from this version.

Figure 6

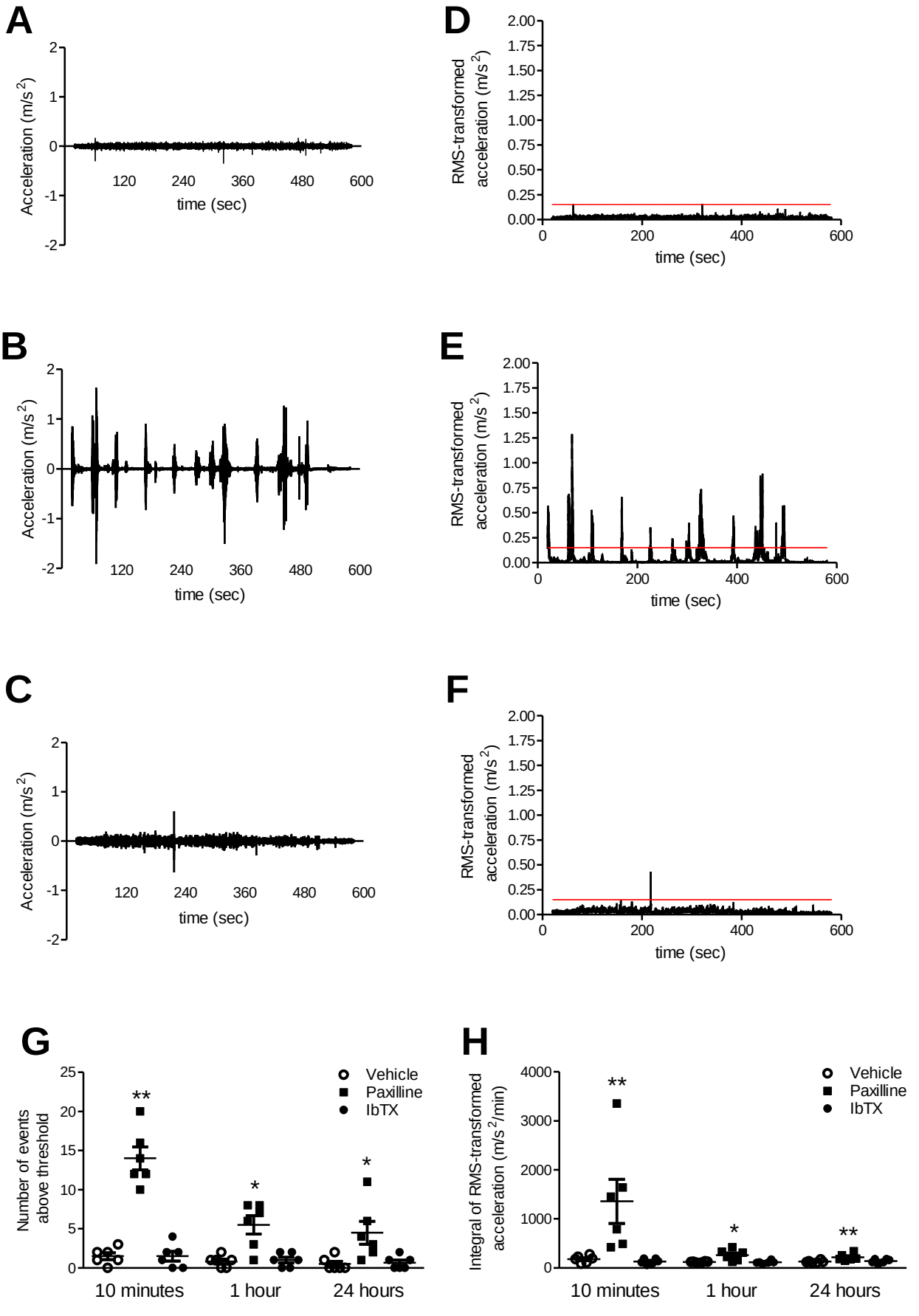

JPET Fast Forward. Published on February 16, 2018 as DOI: 10.1124/jpet.117.245118
This article has not been copyedited and formatted. The final version may differ from this version.

Figure 7